JSR Publications

Available Online

J. Sci. Res. **17** (2), 355-365 (2025)

JOURNAL OF SCIENTIFIC RESEARCH

www.banglajol.info/index.php/JSR

Frequency Dependent Electrical Properties of Hydrogen-Bonded Polymorph Diisopropylammonium Trichloroacetate (dipaTCA)

Ekramul Kabir*

Department of Physics, Darjeeling Govt. College, Darjeeling-734101, West Bengal, India

Received 24 November 2024, accepted in final revised form 11 March 2025

Abstract

The hydrogen-bonded polymorph diisopropylammonium trichloroacetate (dipaTCA) exhibits intriguing electrical properties influenced by frequency-dependent behavior. dipaTCA are generally grown in the bulk by hydrothermal crystallization which produces several high-quality crystals. Frequency and temperature dependence of impedance and modulus spectroscopy, dielectric and ac conductivity are studied in the ranges of 1 kHz-20 MHz at 325-400K respectively. The measurements revealed significant frequency dispersion in both the real and imaginary components of the dielectric constant. The result of the Nyquist plot is found to be fitted with the theoretical Maxwell–Wegner capacitor model. The modulus data suggest that a hopping type mechanism of the system is present here. From the dielectric spectra the maximum value of permittivity $(\varepsilon')_{max}$ is nearly 20 at temperature 387K and frequency 10 kHz. The activation energy (E_a) from the Arrhenius plot is also studied for the conduction mechanism of the material. These findings provide insights into the fundamental electrical properties of dipaTCA, positioning it as a candidate for applications in organic electronics and energy storage devices.

Keywords: Diisopropylammonium cation; Impedance and modulus spectroscopy; Dielectric permittivity; Conductivity.

doi: https://dx.doi.org/10.3329/jsr.v17i2.71999 J. Sci. Res. **17** (2), 355-365 (2025)

1. Introduction

Recently green organic molecular ferroelectric takes the place of inorganic materials, due to its several technological applications in capacitors and electronic devices [1-4]. In the ferroelectric family, the inorganic oxides KH_2PO_4 (KDP) and perovskite-type compounds $PbTiO_3$, $BaTiO_3$, $Pb(ZrTiO_3)$ are widely used in our daily life but have many disadvantages like expensive heavy metal as a constituent, contain toxic lead element, unsuitable for flexible electronics etc. [5-8]. As a result researchers was searching for anew non-toxic ferroelectrics which can be a good alternative of an inorganic one. In the process of searching for new non-toxic ferroelectrics, there are many novel molecular ferroelectrics such as thiourea (CH_4N_2S) [9,10], squaric acid ($C_4H_2O_4$) [11,12], croconic acid [13,14],

* *Corresponding author*: ekramulphysics@gmail.com

TCAA(CCl_3CONH_2) [15,16] etc. have been discovered and studied. However, their low polarization value restricts their application also. But in the year 2011, the first diisopropylammonium based organic molecular ferroelectrics diisopropylammonium chloride (dipaCl) was discovered with high spontaneous polarization 8.2 $\mu C/cm^2$ [17-20]. Two years later, in 2013 another new organic molecular ferroelectric diisopropylammonium bromide (dipaBr) was reported with spontaneous polarization 23 $\mu C/cm^2$ which is comparable to $BaTiO_3$ [21-23]. In the year 2017, a research group from India reported that the spontaneous polarization of another halogen family compound diisopropylammonium iodide (dipaI) is 33 $\mu C/cm^2$ (highest among all organic ferroelectric materials) [24].

This dipa-family forms an interesting group of materials characterized by the presence of hydrogen bonding between $dipa^+$ and X^- ($X=Cl^-$, Br^-, I^- etc.). These types of hydrogen bonds are also responsible for high conductivity [25-27]. In the recent year, an extensive survey of crystal structure was performed on a new organic hydrogen-bonded polymorph diisopropylammonium trichloroacetate ($C_8H_{16}Cl_3NO_2$) (dipaTCA) by a German group [28]. Its hydrogen-bonded network and tunable dielectric behavior suggest its utility in the design of organic materials for flexible electronic devices, such as non-volatile memory storage and sensors. Additionally, dipaTCA's structural adaptability and phase-transition characteristics could make it a candidate for thermal and pressure-sensitive materials in actuators and energy-harvesting systems. Further exploration of its crystallographic properties may also contribute to advancements in supramolecular chemistry and self-assembled nanostructures for targeted functional applications. But no attempt has been made so far to understand the dielectric, impedance, modulus spectroscopy, and ac conductivity in dipaTCA by using impedance or modulus spectroscopy technique. Keeping this in mind, an attempt has been made in this paper for the first time to explain the electrical and dielectric properties of dipaTCA compound as a function of frequency and temperature.

2. Experimental Section

Hydrogen bonded polymers are generally grown in the bulk by hydrothermal crystallization which produces several high-quality crystals. The dipaTCA material was synthesized by using a wet chemical method technique carrying out the reaction between the equal molar amounts of trichloroacetic acid (TCA) and diisopropylamine (dipa) which were purchased from available sources.

These raw materials were mixed with ethanol and on complete dissolution, the solution was left to evaporate to obtain the synthesized salt. After six days a fine transparent colorless needle-like crystals of dipaTCA was obtained by employing slow evaporation of solution growth technique as shown in Fig. 1a-b. Re-crystallizations was done to obtain the single crystal of dipaTCA. These fresh crystals were crushed in an agat mortar, and compressed into tablets of 8 mm in diameter with 1 mm thickness which is shown in Fig. 1c. The pressed pellet sample was subjected to a number of characterizations to study the structural, electrical properties (frequency range 1 kHz-20 MHz and temperature range 325K-400K) and the dielectric studies are performed by using an impedance analyzer.

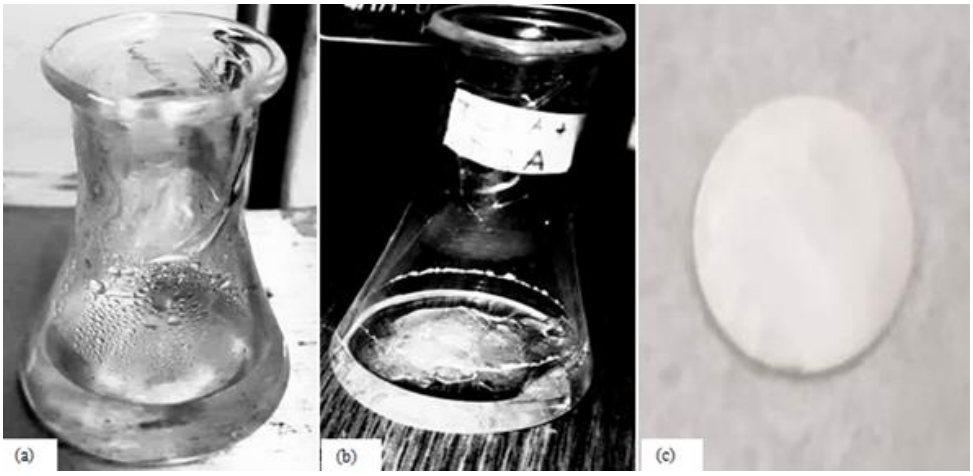

Fig. 1. Formation of dipaTCA at (a) Day-1 and (b) Day-5, (c) Pallet form of the material.

3. Results and Discussion

3.1. *Impedance analysis*

The complex impedance analysis at different temperatures is a powerful approach to analyze the microstructure, electrode effects on the charge transport phenomenon, and various electrical properties. The complex impedance may be explained with the help of an equivalent circuit with resistance and capacitance for the grain and grain boundary according to Maxwell–Wegner capacitor model [29-31].

Fig. 2 shows the Nyquist plot (imaginary part Z'' vs real part Z' of complex impedance) for dipaTCA compound at several temperatures. From this plot, it is clear that the radius of the semicircle decreases with increase in temperature, indicating the existence of activated conduction mechanism [32]. When the temperature is increased, Z'' vs Z' curve changes significantly and at temperature below 350K, there is no semicircle. These plots are fitted with Z-View software and the complex impedance spectrum can be interpreted by an equivalent circuit when the best fit is obtained. We have modeled those spectra by an equivalent circuit made up of a parallel combination of RC circuits connected in series. The RC parameters are extracted from the fitted curve as shown in Fig. 2. The extracted fitted RC parameters at different temperatures are shown in Table 1.

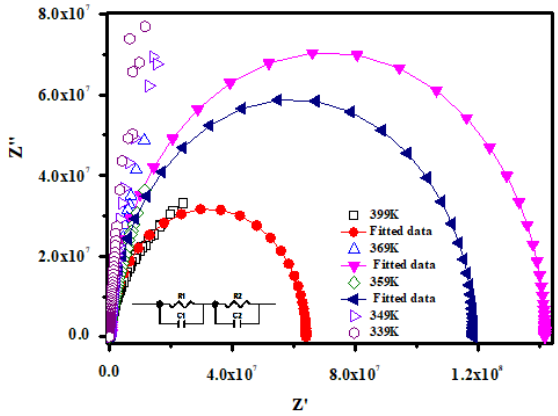

Fig. 2. (color online) Fitted Nyquist plot (Z' vs Z'') of dipaTCA at different temperatures with equivalent circuit.

Table 1. The values of RC parameters at different temperatures.

Temp T(K)	$R_1 \times 10^5$ (Ω)	C_1 (pf)	$R_2 \times 10^7$ (Ω)	C_2 (pf)
399	5.81	2.32	6.35	13.32
369	6.56	1.99	10.13	8.99
359	7.42	1.16	11.78	7.16

Fig. 3a shows the variation of Z' with frequency at different temperatures. From this figure, it is obvious that the magnitude of Z' decreases with the increase in temperature and frequency, which indicates that there is a probability to increase ac conductivity with increasing temperature and frequency [33]. And at higher frequencies all the plots of Z' coincide, indicating a possible release of space charge [34,35]. The variation of Z'' with frequency at different temperatures is shown in Fig. 3(b). From this figure, it is seen that all Z'' merge at higher frequency due to the accession of space charge polarization effect in dipaTCA [36,37].

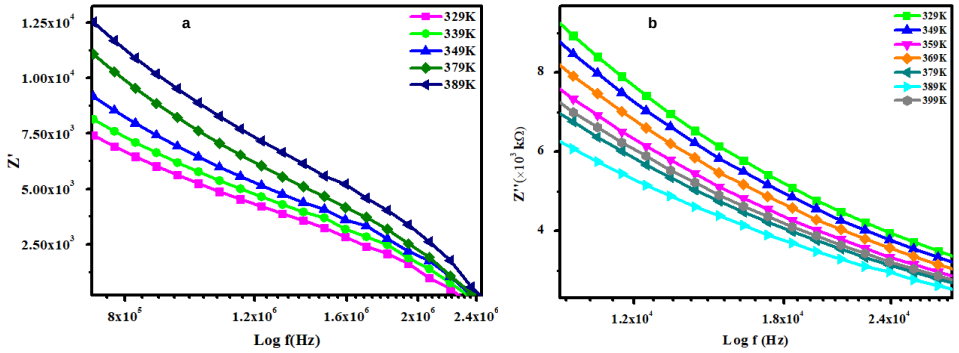

Fig. 3. (color online) (a) Frequency dependence of real part of impedance (Z') of dipaTCA at various temperatures, (b) Frequency dependence of imaginary part of impedance (Z'') of dipaTCA at various temperatures.

3.2. *Complex modulus analysis*

Complex impedance analysis gives more emphasis on the higher resistance elements whereas complex modulus plots highlight on smaller capacitance. Complex modulus spectroscopy is an alternative approach to understand the electrical transport process (relaxation time, ion/carrier hopping rate etc.) as well as it can differentiate electrode polarization from grain boundary conduction processes [38,39]. Hence, it is an important and convenient tool to analyze the dynamic properties of the material. Fig. 4a,b shows the variation of real part of complex modulus M' and imaginary part of complex modulus M'' with frequency at different temperaturesranging from 329K to 399K. In Fig. 4a, M' has low magnitude at lower frequency region, and when frequency increases, the value of M'increases until it reaches almost a constant value at higher temperatures. Also, the value of M' decreases with increasing temperature. Almost similar behavior is shown for all $M'(f)$ plots within experimental temperatures. This indicates that the test material shows a negligible electrode polarization phenomenon [40,41]. As shown in Fig. 4b, the peak height increases with increasing temperatures. With the increasing frequency, the position of the peak shifts to higher temperatures. The peak region indicates the transition from long-range to short-range mobility with increasing frequency. This type of behavior is known as temperature-dependent hopping type mechanism of the system [42-46]. So, the result of the modulus spectrum suggests that at an elevated temperature, there exists a hopping mechanism due to the difference in the charge carriers, that leads to the electrical conductivity.

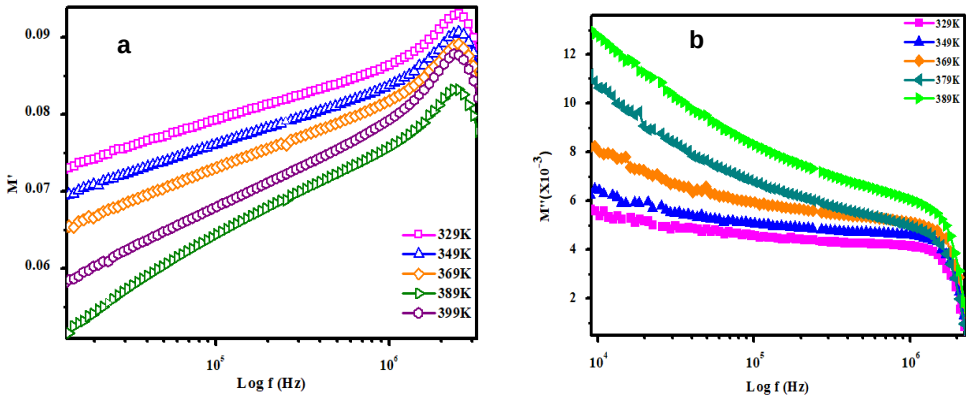

Fig. 4. (color online) (a) Frequency dependence of real part of modulus ($\boldsymbol{M'}$) at different temperatures, (b) Frequency dependence of imaginary part of modulus ($\boldsymbol{M''}$) at different temperatures.

3.3. *Dielectric studies*

Complex dielectric permittivity is another important root of information to investigate about electrical and dielectric properties. Physically, the real part (ε') and imaginary part (ε'') of permittivity represent the charging and the loss current respectively [47-49]. Here ε'

identifies the energy stored in the material from the applied electric field and also the strength of alignment of dipoles. The term ε'' (or loss factor) is the energy dissipated in the material associated with the frictional damping.

The variation of ε' and ε'' as a function of frequency with different temperatures are shown in Fig. 5. It is observed that at lower frequencies both ε' and ε'' have large values that decrease with increase in frequency and attains a constant limiting value due to free dipole swing in a dielectric medium in the presence of an alternating electric field [50]. It can also be concluded from the graph that when the temperature is high and frequency is low both ε' and ε'' have strong temperature variation. At lower frequency all the dipoles follow the electric field and the high value of ε' arises due to the accumulation of charges at the interfaces between the material and the electrode and at grain boundaries, it follows the Maxwell-Wagner (M-W) model [51-53]. When frequency increases, all dipoles begin to lag behind the field and ε' slightly decreases. At very higher frequencies the dipoles can no longer follow the electric field. A typical plot of ε' versus temperature at various frequencies is shown in Fig. 6. From this figure, it can be observed that at temperature 373K the dielectric permittivity is 15.5 and the maximum value of permittivity $(\varepsilon')_{max}$ at temperature

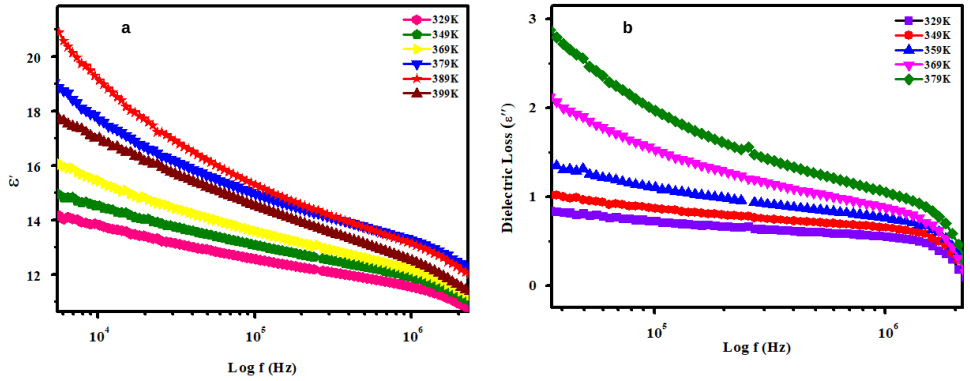

Fig. 5. (color online) (a) Frequency dependence of real part of permittivity (ε′) of dipaTCA at various temperatures, (b) Frequency dependence of Imaginary part of permittivity (ε′′) of dipaTCA at various temperatures.

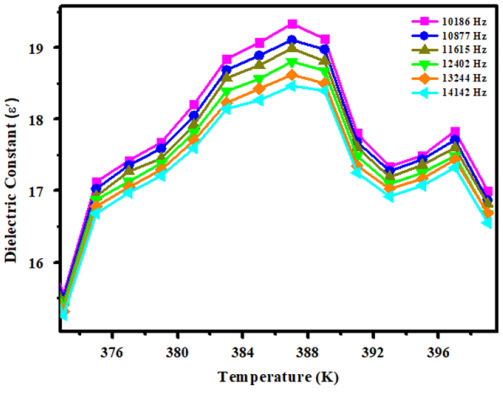

Fig. 6. (color online) Temperature dependence of dielectric permittivity at different frequency.

3.4. *Conductivity analysis*

Frequency and temperature-dependent conductivity is a well-known method for characterizing the hopping dynamics of dipaTCA. To explain the mechanism, the frequency dependence of conductivity at different temperatures is depicted in Fig. 7. The temperature variation of ac conductivity is shown in Fig. 8. From the frequency-dependent ac conductivity curve it is clear that σ_{ac} increases with increasing temperature due to the presence of impurities or dislocations at metal-semiconductor interface and these impurities lie below the bottom of the conduction band, resulting in small activation energy (E_a) [54-58]. At strongly frequency- dependent region, the hopping of the charge carriers among the trap level in the band gap dominated the transport [59-63]. By an empirical relation ac conductivity is related to E_a and the inverse absolute temperature (T):

$$\sigma_{ac} = \sigma_0 exp\left(-\frac{E_a}{K_B T}\right) \quad (1)$$

Where σ_0 is the pre-exponential factor of ac conductivity, K_B=Boltzman constant and E_a is the activation energy. From the Arrhenius plot (log σ_{ac}vs. 1000/T) of ac conductivity, E_a is calculated by fitting the straight line and the value is found to be 0.28 eV. This low value of E_a suggests that the conduction mechanism may be due to the hopping of electrons [64-66].

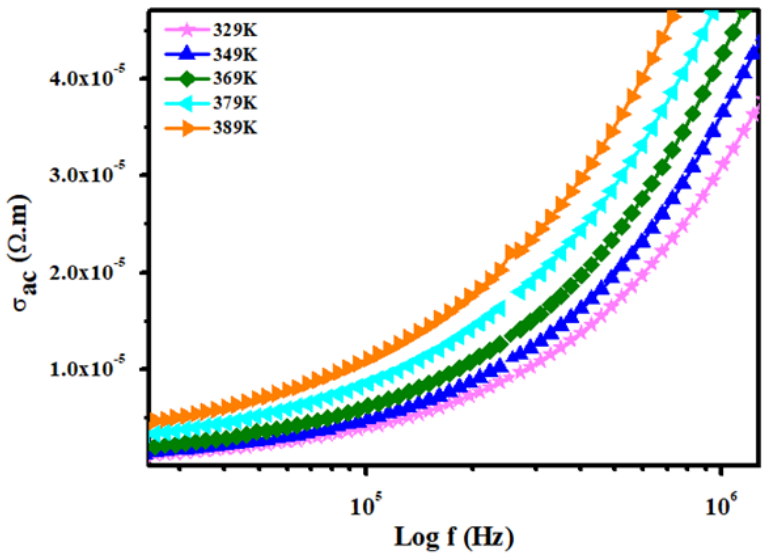

Fig. 7. (color online) Experimental curve of ac conductivity as a function of frequency at different temperatures.

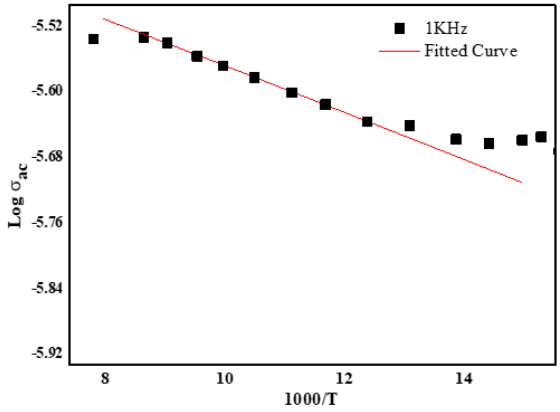

Fig. 8. (color online) Variation of ac conductivity with temperature.

4. Conclusion

Frequency and temperature-dependent electrical parameters e.g impedance, modulus, dielectric constant and ac conductivity have been investigated within a broad range of frequency. The Nyquist plot can be interpreted from well- fitted RC parameters with the help of an equivalent circuit model with resistance and capacitance for the grain and grain boundary in consonance with Maxwell–Wegner capacitor model. Furthermore, the value of M' decreases with increasing temperature, indicates that the material shows a negligible electrode polarization phenomenon. The frequency-dependent M'' suggest that there is a transition from long range to short-range mobility, indicating a hopping mechanism of the system. From the dielectric spectra, it is seen that at temperature 373K the dielectric permittivity is 15.5 and the maximum value of permittivity $(\varepsilon')_{max}$ at temperature 387K reaches ≈ 20 (both measured at frequency 10kHz). The activation energy (E_a) is calculated by fitting the Arrhenius plot of ac conductivity and it is 0.28eV, which suggests that the conduction mechanism may be due to the hopping of electrons.

Acknowledgment

The author is grateful to M. Khatun, New Integrated Govt School (E.M), Raiganj for material preparation and data collection process.

References

1. J. F. Scott, Science **315**, 954 (2007). https://doi.org/10.1126/science.1129564
2. H. Anetai, K. Sambe, T. Takeda, N. Hoshino, and T. Akutagawa, Chem. -A Eur. J. **25**, 11233 (2019). https://doi.org/10.1002/chem.201902544
3. H. Zhu, C. Fu, and M. Mitsuishi, Polym. Int. **70**, 404 (2021). https://doi.org/10.1002/pi.6029
4. M. Khatun and E. Kabir, Solid State Comm. **400**, ID 115897 (2025). https://doi.org/10.1016/j.ssc.2025.115897

5. G. Busch and P. Scherrer, Naturwissenschaften **23**, 737 (1935). https://doi.org/10.1007/BF01498152
6. G. H. Haertling, J. Am. Ceram. Soc. **82**, 797 (1999). https://doi.org/10.1111/j.1151-2916.1999.tb01840.x
7. M. E. Lines and A. M. Glass, Principles and Applications of Ferroelectrics and Related Materials (Clarendon Press, Oxford, 1977).
8. Alisha and D. Garg, J. Sci. Res. **16**, 2 (2024). https://doi.org/10.3329/jsr.v16i2.68155
9. A. L. Solomon, Phys. Rev. **104**, 1191 (1956). https://doi.org/10.1103/PhysRev.104.1191
10. H. Futama, J. Phys. Soc. Japan **17**, 434 (1962). https://doi.org/10.1143/JPSJ.17.434
11. D. Semmingsen and J. A. Feder, Solid State Comm. **15**, 1369 (1974). https://doi.org/10.1016/0038-1098(74)91382-9
12. S. Horiuchi and Y. Tokura, Nature Mater. **7**, 357 (2008). https://doi.org/10.1038/nmat2137
13. S. Horiuchi, Y. Tokunaga, G. Giovannetti, S. Picozzi, H. Itoh, R. Shimano, and Y. Tokura, Nature **463**, 789 (2010). https://doi.org/10.1038/nature08731
14. D. A. Kunkel, J. Hooper, S. Simpson, G. A. Rojas, S. Ducharme, T. Usher, E. Zurek, and A. Enders, Phys. Rev. B **87**, ID 041402 (2013). https://doi.org/10.1103/PhysRevB.87.041402
15. M. Hashimoto, A. Shono, Y. Mido, H. Niki, H. Hentona, and K. Mano, Verlag der Zeitschrift fur Naturforschung **45A**, 327 (1990). https://doi.org/10.1515/zna-1990-3-419
16. Y. Kamishina, Y. Akishige, and M. Hashimoto, J. Phys. Soc. Japan **60**, ID 2147 (1991). https://doi.org/10.1143/JPSJ.60.2147
17. D. W. Fu, W. Zhang, H. L. Cai, J. Z. Ge, Y. Zhang, and R.G. Xiong, Adv. Mater. **23**, 5658 (2011). https://doi.org/10.1002/adma.201102938
18. S. V. Baryshnikova, E. V. Charnayac, A. Y. Milinskiya, V. A. Parfenovd, and I. V. Egorova, Phase Transitions **91**, 293 (2018). https://doi.org/10.1080/01411594.2017.1378880
19. N. I. Uskova, E. V. Charnaya, D. Y. Podorozhkin, S. V. Baryshnikov, I. V. Egorova, and A. Y. Milinskiy, Phys. Solid State **62**, 1195 (2020). https://doi.org/10.1134/S1063783420070264
20. M. Khatun and E. Kabir, J. Adv. Dielectrics **11**, ID 2150015 (2021). https://doi.org/10.1142/S2010135X21500156
21. D. W. Fu, H. L. Cai, Y. Liu, Q. Ye, W. Zhang, Y. Zhang, X. Y. Chen, G. Giovannetti, M. Capone, J. Li, and R. G. Xiong, Science **339**, 425 (2013). https://doi.org/10.1126/science.1229675
22. M. Khatun and E. Kabir, Solid State Comm. **393**, ID 115670 (2024). https://doi.org/10.1016/j.ssc.2024.115670
23. A. Piecha, A. Gagor, R. Jakubas, and P. Szklarz, Cryst. Eng. Comm. **15**, 940 (2013). https://doi.org/10.1039/C2CE26580J
24. R. K. Saripalli, D. Swain, S. Prasad, H. Nhalil, H. L. Bhat, T. N. G. Row, and S. Elizabeth, J. Appl. Phys. **121**, 114101 (2017). https://doi.org/10.1063/1.4978515
25. R. Pepinsky, K. Vedam, Y. Okaya, and S. Hoshino, Phys. Rev. **111**, ID 1508 (1958). https://doi.org/10.1103/PhysRev.111.1508
26. R. Pepinsky and K. Vedam, Phys. Rev. **117**, ID 1502 (1960). https://doi.org/10.1103/PhysRev.117.1502
27. M. Khatun and E. Kabir, J. Mater. Sci.: Mater. Elect. **35**, 2091 (2024). https://doi.org/10.1007/s10854-024-13845-1
28. G. J. Reiss, M. K. Meyer, and J. Graf, Z. Kristallogr. NCS **234**, 875 (2019). https://doi.org/10.1515/ncrs-2019-0064
29. N. G. McCrum, B. E. Read, and G. Williams, Anelastic and Dielectric Effects in Polymeric Solids (Wiley, New York, 1967) pp. 617. https://doi.org/10.1002/app.1969.070130214
30. S. Mahboob, G. Prasad, G.S. Kumar, Bull. Mater. Sci. **29** 347 (2006). https://doi.org/10.1007/BF02704134
31. I. Shubashini and S. R. Jebas, J. Sci. Res. **17**, 1 (2025). https://doi.org/10.3329/jsr.v17i1.74784
32. T. Collins, Optical and Digital Image Processing: Fundamentals and Applications, ed. G. Cristobal et al. (Wiley-VCH Verlag GmbH & Co. KGaA, 2011) pp. 859. https://doi.org/10.1002/9783527635245

33. S. Selvasekarapandian and M. Vijaykumar, Mater. Chem. Phys. **80**, 29 (2003). https://doi.org/10.1016/S0254-0584(02)00510-2
34. J. Plocharski and W. Weiczorek, Solid State Ionics **28**, 979 (1988). https://doi.org/10.1016/0167-2738(88)90315-3
35. E. V. Hauff, J. Phys. Chem. C **123**, 11329 (2019). https://doi.org/10.1021/acs.jpcc.9b00892
36. K. P. Chandra, K. Prasad, and R. N. Gupta, Physica B: Condensed Matter **388**, 118 (2007). https://doi.org/10.1016/j.physb.2006.05.010
37. V. Purohit, R. N. P. Choudhary, and A. Sahoo, Mater. Res. Express **6**, 125710 (2019). https://doi.org/ 10.1088/2053-1591/ab771d
38. A. V. Sarode and A. C. Kumbharkhane, J. Mol. Liq. **164**, 226 (2011). https://doi.org/10.1016/j.molliq.2011.09.020
39. G. C. Psarras, E. Manolakaki, and G. M. Tsangaris, Composites Part A **34**, 1187 (2003). https://doi.org/10.1016/j.compositesa.2003.08.002
40. M. Sural and A. Ghosh, J. Phys. Condensed Matter **10**, 10577 (1998). https://doi.org/10.1088/0953-8984/10/47/009
41. A. Rouahi, A. Kahouli, F. Challali, et al, J. Phys. D: Appl. Phys. **46**, ID 065308 (2013). https://doi.org/ 10.1088/0022-3727/46/6/065308
42. K. Prabakar, S. K. Narayandass, and D. Mangalaraj, Phys. Stat. Sol. **199**, 507 (2003). https://doi.org/10.1002/pssa.200306628
43. A. K. Jonscher, Universal Relaxation Law (Chelsea Dielectric Press, London, 1996). https://doi.org/10.1088/0022-3727/32/14/201
44. F. Yakuphanoğlu, Physica B **393**, 139 (2007). https://doi.org/10.1016/j.physb.2006.12.075
45. T. Z. Rizvi and A. Shakoor, J. Phys. D: Appl. Phys. **42**, ID 095415 (2009). https://doi.org/10.1088/0022-3727/42/9/095415
46. M. Ram and S. Chakrabarti, J. Alloys Compd. **462**, 214 (2008). https://doi.org/10.1016/j.jallcom.2007.08.001
47. A. Eroğlu, A. Tataroğlu, and S. Altındal, Microelectron. Eng. **91**, 154 (2012). https://doi.org/10.1016/j.mee.2011.07.016
48. M. M. A. Kader, M. Y. Elzayat, T. R. Hammad, A. I. Aboud, and H. Abdelmonem, Phys. Scr. **83**, ID 035705 (2011). https://doi.org/10.1088/0031-8949/83/03/035705
49. Mubasher and M. Mumtaz, J. Alloys Compd. **866**, ID 158750 (2021). https://doi.org/10.1016/j.jallcom.2021.158750
50. M. Bourguiba, Z. Raddaoui, A. Dhahri, M. Chafra, J. Dhahri, and M. A. Garcia, J. Mater. Sci.: Mater. Electron. **31**, 11810 (2020). https://doi.org/10.1007/s10854-020-03733-9
51. K. S. Rao, P. M. Krishna, D. M. Prasad, J. H. Lee, and J. S. Kim, J. Alloys Compds. **464**, 49 (2008). https://doi.org/10.1016/j.jallcom.2007.10.023
52. H. Frohlieh, Theory of Dielectrics (Oxford University Press, London, 1958).
53. D. O'Neill, R. M. Bowman, and J.M. Gregg, Appl. Phys. Lett. **77**, 1520 (2000). https://doi.org/10.1063/1.1290691
54. S. Maity, D. Bhattacharya, and S.K. Ray, J. Phys. D: Appl. Phys. **44**, ID 095403 (2011). https://doi.org/10.1088/0022-3727/44/9/095403
55. A. K. Dubey, P. Singh, S. Singh, D. Kumar, and O. Parkash, J. Alloys Compd. **509**, 3899 (2011). https://doi.org/10.1016/j.jallcom.2010.12.156
56. M. A. Elkestawy, S. A. kader, and M. A. Amer, Physica B **405**, 619 (2010). https://doi.org/10.1016/j.physb.2009.09.076
57. R. Amin, K. Samantaray, E. G. Rini, I. Bhaumik, and S. Sen, Ceram. Inter. **47**, 13118 (2021). https://doi.org/10.1016/j.ceramint.2021.01.176
58. A. M. Farid, H. E. Atyia, and N. A. Hegab, Vacuum **80**, 284 (2005). https://doi.org/10.1016/j.vacuum.2005.05.003
59. A. Eroğlu, A. Tataroğlu, and S. Altındal, Microelectron. Eng. **91**, 154 (2012). https://doi.org/10.1016/j.mee.2011.07.016
60. W. Masmoudi, S. Kamoun, and M. Gargouri, Ionics **18**, 117 (2012). https://doi.org/10.1007/s11581-011-0601-z

61. S. Hajra, M. Sahu, V. Purohit, and R. N. P. Choudhary, Heliyon **5**, ID e01654 (2019). https://doi.org/10.1016/j.heliyon.2019.e01654
62. K. C. Verma, M. Ram, J. Singh, and R.K. Kotnala, J. Alloys Compd. **509**, 4967 (2011). https://doi.org/10.1016/j.jallcom.2011.01.144
63. L. Agrawal, A. Dutta, S. Shannigrahi, B. P. Singh, and T. P. Sinha, Physica B **5**, 406 (2011). https://doi.org/10.1016/j.physb.2010.12.043
64. B. Louati, F. Hlel, and K. Guidara, J. Alloys Compd. **486**, 299 (2009). https://doi.org/10.1016/j.jallcom.2009.06.148
65. A. Hegab, M. A. Afifi, H. E. Atyia, and A. S. Farid, J. Alloys Compd. **477**, 925 (2009). https://doi.org/10.1016/j.jallcom.2008.11.129
66. A. E. Bachiri, M. E. Hasnaoui, A. Louardi, A. Narjis, and F. Bennani, Physica B: Cond. Matt. **571**, 181 (2019). https://doi.org/10.1016/j.physb.2019.07.002